Conclusions

An analysis has been developed for high-aspect-ratio jet-flap wings of arbitrary geometry and blowing. It appears that the present method is as accurate as other known methods and is flexible and rapid, particularly for discontinuous planforms. Although definitive test data are lacking, correlation with existing experimental data is satisfactory. To properly evaluate jet-flap theories, it is recommended that definitive lifting-surface analyses be developed and properly controlled and corrected experiments conducted, including cases with discontinuous parameters. Finally, it is believed that the present method is a useful analytical tool for jet-flap wing design.

References

[1]Maskell, E. C., and Spence, D. A. "A Theory of the Jet Flap in Three Dimensions," *Proceedings of the Royal Society (London)*, Ser. A, Vol. 251, No. 1266, June 9, 1959, pp. 407–425.

[2]Spence, D. A., "The Lift Coefficient of a Thin, Jet-Flapped Wing," *Proceedings of the Royal Society (London)*, Ser. A, Vol. 238, No. 1212, Dec. 4, 1956, pp. 46–48.

[3]Lissaman, P. B. S., "A Linear Theory for the Jet Flap in Ground Effect," *AIAA Journal*, Vol. 6, No. 7, July 1968, pp. 1356–1362.

[4]Huckemann, D., "A Method of Calculating the Pressure Distribution over Jet Flapped Wings," R & M 3036, British Aeronautical Research Council, London, 1957.

[5]Hartunian, R. A., "The Finite Aspect Ratio Jet Flap," CAL Rept. A1-1190-A-3, Oct. 1959, Cornell Aeronautical Lab., Buffalo, N.Y.

[6]Kerney, K. P., "A Theory of the High Aspect Ratio Jet Flap," *AIAA Journal*, Vol. 9, No. 3, March 1971. pp. 431–435.

[7]Tokuda, N., "An Asympototic Theory of the Jet Flap in Three Dimensions," *Journal Fluid Mechanics*, Vol. 46, Pt. 4, April 27, 1971, pp. 705–726.

[8]Lopez, M. L. and Shen, C. C.," Recent Developments in Jet Flap Theory and Its Application to STOL Aerodynamic Analysis," AIAA Paper 71-578, 1971, Palo Alto, Calif.

[9]Lissaman, P. B. S., "Analysis of High-Aspect-Ratio Jet Flap Wings of Arbitrary Geometry," CR-2179, 1973, NASA.

[10]Multhopp, H., "The Calculation of the Lift Distribution of Aerofoils," R. T. P. Translation 2392, British Ministry of Aircraft Production, London.

[11]Glauert, H., *The Elements of Airfoil and Airscrew Theory*, Cambridge University Press, 2nd ed. 1948.

[12]Williams, J. and Alexander, A. J., "Three-Dimensional Wind-Tunnel Tests of a 30° Jet Flap Model," Conference Paper 304, British Aeronautical Research Council, London, 1957.

MAY 1974 J. AIRCRAFT VOL. 11, NO. 5

Aircraft Wake Vortex Transport Model

M. R. Brashears*
Lockheed Missiles & Space Company, Inc., Huntsville, Ala.
and
James N. Hallock†
DOT/Transportation Systems Center, Cambridge, Mass.

A wake vortex transport model has been developed which includes the effects of wind and wind shear, buoyancy, mutual and self-induction, ground plane interaction, viscous decay, finite core and Crow instability effects. Photographic and ground-wind vortex tracks obtained from DC-6, B-747, B-707, and CV-880 aircraft flybys are compared with predicted vortex tracks computed using meteorological and aircraft data as inputs to the transport model. A parametric analysis of the effects of the aircraft, fluid mechanic, and meteorological parameters shows the relative magnitude of each transport mechanism. The study constitutes the first detailed comparison of vortex transport theory with experimental data.

I. Introduction

AIRCRAFT wakes have long been recognized as safety and airport utilization problems. However, with the introduction of the large transport aircraft (B-747, DC-10, L-1011) and the ever increasing airport congestion, the wake vortex problem has taken on added significance. The vortices from large aircraft can present a severe hazard to other aircraft which inadvertently encounter the vortices; the following aircraft can be subjected to rolling moments which exceed the aircraft's roll control authority, to a dangerous loss of altitude, and to a possible structural failure. The probability of an aircraft-vortex encounter is greatest in the terminal area where light and heavy aircraft operate in close proximity and where recovery from an upset may not be possible due to the low aircraft altitude. To prevent aircraft-vortex encounters, the present solution (implemented by the Federal Aviation Administration in March 1970) has been to increase the separation standards behind the heavy jets. However, these increased separations decrease the capacity of the airport system and the present and predicted demands on airports cannot be met by just constructing additional runways and airports. Airport and airway system utilization are projected to double by 1980 and to increase five-fold by 1995. Technologically (using dual runways, improved landing aids, etc.), runway capacity can be substantially increased today, but not until the wake vortex problem and the inherent safety aspects have been alleviated.

There are two primary approaches to the wake vortex

Presented as Paper 73-679 at the AIAA 6th Fluid and Plasma Dynamics Conference, Palm Springs, Calif., July 16–18, 1973; submitted July 26, 1973; revision received January 23, 1974. The authors thank D. Burnham and T. Sullivan of TSC for providing the vortex tracking data prior to publication, K. Shrider of Lockheed-Huntsville for programing the model, and L. Garodz and N. Miller of NAFEC for providing their support during the testing and in the reduction of the rawinsonde and tower data.

Index category: Jets, Wakes, and Viscid-Inviscid Flow Interactions.

*Scientist Associate Research, Fluid Mechanic Applications Group. Member AIAA.

†Developmental Engineer, Wake Vortex Program. Member AIAA.

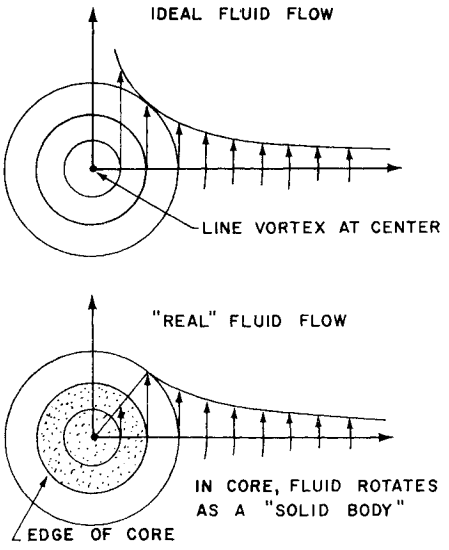

Fig. 1 Comparison of ideal and "real" flowfields for two-dimensional flow about a vortex.

problem which are currently underway. NASA is concentrating on methods to hasten the demise of vortices at the source by modifying the aircraft. Among the many concepts being investigated are wing spoilers, mass injection, wing-tip modifications, and the deployment of trailing devices. These concepts, if they can be shown to economically and effectively reduce the vortex hazard, may not be available in the near future and would still entail a massive retrofit program to alter the current fleet of transport aircraft. For future generation aircraft, NASA is examining the efficacy of aircraft design changes such as mounting engines at the wing tips and tailoring the wing design to cause the vortices to burst quickly.

Concurrently, the FAA/Transportation System Center (TSC) approach to the vortex problem has been to develop systems which use meteorological sensors and/or vortex tracking sensors to provide safe spacing between aircraft and to issue a warning should a hazardous condition exist or be forecast. This approach is predicated on the observation that the separation criteria are conservative most of the time as they ignore conditions such as strong crosswinds which will cause the vortices to dissipate rapidly or blow clear of the path of a following aircraft. Measurements have shown that vortices rarely remain stationary and do not persist indefinitely. The frequency of occurrence of an aircraft-vortex encounter can be shown to be small; traffic is thus unnecessarily delayed by always adhering to the present inflexible regulations.

A warning system is being implemented[1] which provides a protected region in the approach corridor of a runway by constantly monitoring the corridor with vortex tracking sensors. More advanced systems will require the ability to forecast vortex motions and decay. A simple vortex predictive system has been recently proposed[2] but has not been validated. Preliminary results of forecasting the decay of vortices have been reported by Tombach[3] who conducted flight experiments with smoke-marked vortices from a Cessna 170 and correlated the time-to-linking of the vortex pair and vortex bursting with the ambient turbulence level. A new analysis[4] for the Crow instability[5] expresses the time-to-linkage as an explicit function of the turbulence dissipation rate and is corroborated by the limited flight test data.

To develop a model for the transport of the vortex pair, fluid mechanic representations of the various vortex-induced and atmospheric effects have been combined into a unified computer simulation. A series of flight tests using B-747, B-707, DC-6, and CV-880 aircraft was done at the

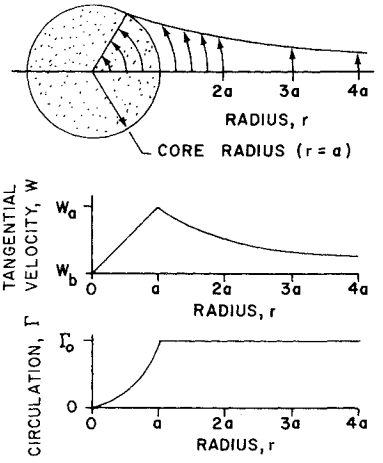

Fig. 2 Rankine vortex (two-dimensional model).

National Aviation Facilities Experimental Center (NAFEC), Atlantic City, N. J., in which both the motion of the vortices and the attendant meteorological conditions were recorded. The tests were conducted to examine a simple transport model and to extend the model by a parametric analysis of the ambiguities between the measured and predicted vortex motions.

II. Transport Model

Fundamentals of Vortex Motion

The idealized flow about a circular vortex consists of an inverse radial velocity distribution (see Fig. 1); but this predicts an infinite velocity at the vortex center. However, in reality, the vorticity is not concentrated at a point but is distributed over some nonzero area. The fluid in this area (the core) moves like a rigid body rotating about the center of the vortex (Fig. 1). The vortex has a velocity field with the magnitude at any point called the induced velocity. (It is customary to refer to this velocity as induced by the vortex but it should be noted that this is merely a representation and that actually it is the velocity that would coexist with the vortex in an otherwise undisturbed fluid.)

The transport model approximates the aircraft vortices by two free vortices with finite cores. The induced velocity field of each vortex is shown in Fig. 2 along with the distribution of circulation (vorticity). The defining equations are derived by equating the static pressure distribution to the centrifugal acceleration with the results given in the figure. The instantaneous streamlines of the flowfield due to a vortex pair are shown in Fig. 3a while the relative streamlines produced by the sinking motion are shown in Fig. 3b. Neither vortex induces any motion to itself; thus the sink velocity is given by

$$w_s = (-\Gamma/2\pi b')$$

where Γ is the circulation or "strength" of the vortex and b' is the instantaneous separation of the vortex pair. A limiting streamline exists and that fluid inside the oval defined by the streamline travels with the vortices in the absence of mixing. The size and shape of the oval can be calculated from potential flow theory[6] and is found to be nearly elliptical and of area

$$A \cong 11.42(b'/2)^2$$

To establish the transport of the vortex pair, the relationships of the defining parameters to the generating aircraft must be found. This can be done by relating the final conditions of the rollup process to the aircraft parameters and using these values as initial conditions.

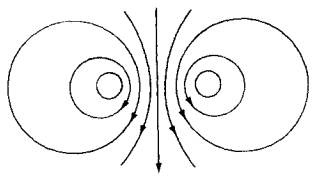

INSTANTANEOUS STREAMLINES
DUE TO A VORTEX PAIR

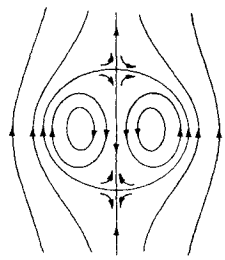

STEADY STREAMLINES
DUE TO A VORTEX PAIR

Fig. 3 Streamlines of a vortex pair.

The circulation loading distribution of a wing defines all the properties of the inviscid vortex development; however, at the present stage of the transport model development, it is merely assumed that an organized vortex pair motion exists. The pair moves in its induced field causing the vortices to convect downward with a velocity directly proportional to the aircraft lift coefficient and velocity and inversely proportional to the aspect ratio. Using classical dynamics and the elliptic lift approximations,[7] the initial wake can be classified by

$$\Gamma = (4W/\pi\rho V b)$$

where W is the aircraft weight, ρ is the air density, V is the aircraft speed, and b is the wingspan. Accordingly, the initial vortex spacing will be

$$b' = (\pi/4)b$$

The aircraft weight, flight speed, and wingspan are thus the only aircraft parameters used. The effect of flaps can be considered by replacing the wingspan b with an effective wingspan b''; larger flap settings alter the load distribution by concentrating the load distribution more inboard and thus $b'' < b$.

Ground Effect

Next to the local wind, the ground effect is the most important mechanism affecting the transport of the vortices and is readily calculated by using the image system of classical hydrodynamical theory.[6] For two-dimensional line vortices, the velocity of any one vortex is due solely to the remaining vortices (real and image) in the system.

For the general case consider the vortex pair to be located symmetrically about the z-axis at altitudes z_1 and z_2 as shown in Fig. 4. Let each vortex have an image of equal strength at $-z_1$ and $-z_2$, respectively. The transport of vortex A is given by

$$y_A = V_B\frac{(z_1 - z_2)}{r_B} - V_C\frac{(z_1 + z_2)}{r_C} + V_D$$

$$\dot{z}_A = V_C\frac{2y}{r_C} - V_B\frac{2y}{r_B}$$

and is determined by resolving the induced velocity by each vortex into horizontal and vertical components.

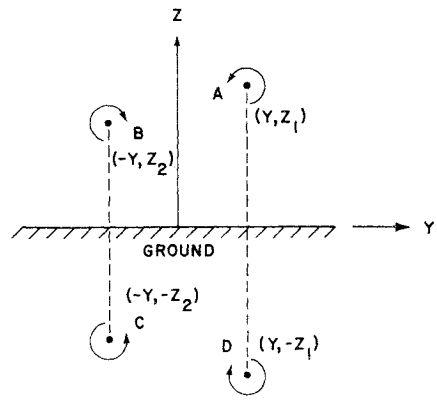

Fig. 4 Vortex image system for ground plane interaction.

The speed induced at any point is given by the inverse distance law, and its direction is perpendicular to the line adjoining the two points

$$V_B = (\Gamma/2\pi r_B)$$

$$V_C = (\Gamma/2\pi r_C)$$

$$V_D = (\Gamma/2\pi r_D)$$

where

$$r_B = [(z_1 - z_2)^2 + 4y^2]^{1/2}$$

$$r_C = [(z_1 + z_2)^2 + 4y^2]^{1/2}$$

$$r_D = 2z_1$$

When the initial altitudes are the same, it is readily seen that the equations reduce to the well-known motion of a vortex filament parallel to two perpendicular planes (the axis of symmetry and the ground). The initial sink velocity is determined by the instantaneous separation of the wake vortices; thus the motion of vortices created just above an altitude of $b'/2$ will travel as if they were initially created at a separation somewhat less than b'. If, however, the vortices are created at an altitude less than b', the initial horizontal velocity will be greater and the spreading will occur more rapidly than in the previous case. The vortices will then descend to an altitude less than that corresponding to $\pi b/8$.

Wind and Wind Shear

The effect of a wind field on the transport of the vortex pair can be calculated by superimposing the wind vortex on the existing motion. This vector is defined in terms of the magnitude and azimuth at various altitudes for the horizontal portion and with a variable vertical component. This is in effect assuming that the wind merely has a translating effect upon the mass of air contained in the oval.

The concept of wind shear is included to explain trends known to exist from experiment. The downwind vortex often rises after encountering the ground plane and this can be understood by considering the pressure gradients that flow in the boundary layer. The sinking oval containing the aircraft vortices produces a relative flowfield about its boundary. In the presence of a ground plane, cross flow in the Earth's boundary layer begins to operate against an adverse pressure gradient beneath the pair. As the vortex transport brings the pair closer to the ground, this adverse pressure gradient may become strong enough to separate the flow producing a bubble containing vorticity opposite in sense to the downwind aircraft vortex. Harvey and Perry[8] depicted the bubble as growing rapidly in the downwind direction and finally detaching from the surface as a secondary vortex fed by a vortex sheet from

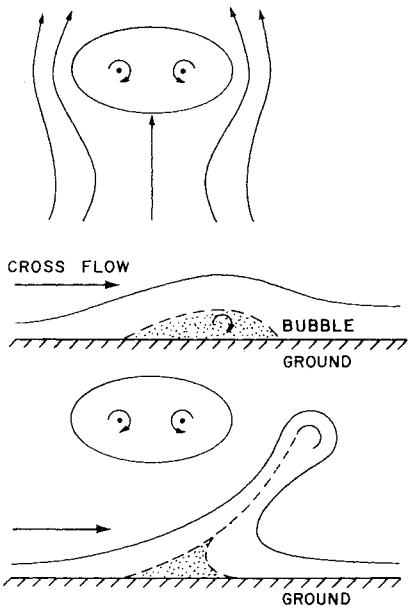

Fig. 5 Schematic of wind shear (from Ref. 8).

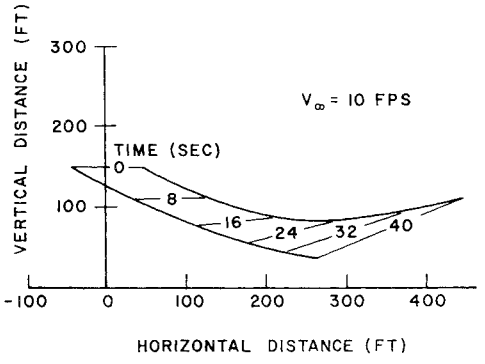

Fig. 6 Transport path for vortex pair in wind shear.

the separation point. This secondary vortex induces an upward component to the total induced velocity field, thus causing the downwind vortex to rise. This is shown schematically in Fig. 5.

Burnham[9] has suggested modeling this phenomenon by simulating the shear layers by rows of discrete vortices where all of the vorticity in the Earth's boundary layer is contained within these vortices. An image system of identical vortices is used to satisfy the boundary condition of no vertical wind component at the surface. The system of shear vortices can be described in terms of any number of vortices per row and any number of rows (plus the corresponding images). The magnitude of the circulation of each vortex is calculated from the geostrophic wind condition and this value can be distributed over the boundary layer in any fashion by assigning each row a fractional strength corresponding to the desired distribution.

The general effect of using wind shear vortices is shown in Figs. 6–8. Figure 6 shows the effect of the wind shear with all of the vorticity concentrated in one row at an altitude of 30 ft with a spacing of 50 ft between the discrete vortices. It is seen that the downwind vortex does indeed rise while no apparent difference is noted in the upwind vortex motion. Figure 7 depicts the effect of changing the number *(I)* of shear layers (rows) where each row has equal fractional strength *(F)*. Again, the upwind vortex path is essentially unchanged. However, the downwind vortex transport shows a rising trend that is weakly dependent on the number of rows. A single row is noted to produce the largest change for a given instant of time.

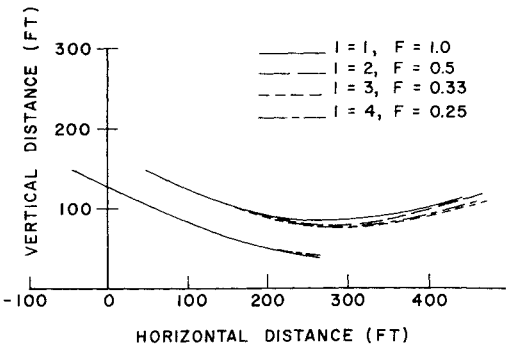

Fig. 7 Comparison of the effect of the number of rows on transport path.

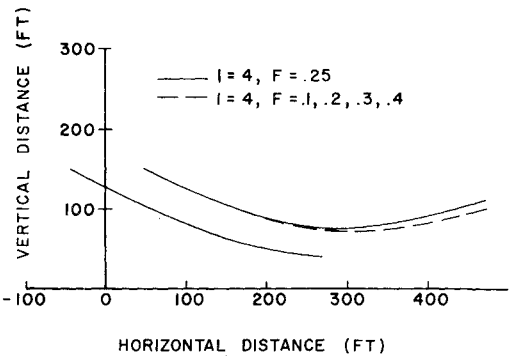

Fig. 8 Comparison of the effect of the vorticity distribution on transport path.

The effect of distributing the vorticity within the shear layer on the motion is shown in Fig. 8 where the largest fractional strength (0.4) is contained in the row nearest the ground.

Buoyancy

The vertical descent of the vortex wake is expected to vary as a function of atmospheric conditions and there are indications that buoyancy may be a significant factor. The driving force for producing changes in the initial motion is a result of the difference in density created during the descent of the pair through a stratified fluid. Even for the case of no initial density difference (no engine exhaust entrainment), a difference is produced if the nearly adiabatic compression of the oval (due to increasing atmospheric density) is different from the stratification of the atmosphere. The resulting density difference produces a buoyant force that affects the vertical momentum of the vortex pair. Buoyancy generated in this manner alters the circulation[10]; however, the manner of alteration has not been established. Tombach[11] maintains that the buoyancy generated vorticity is entrained through mixing of the ambient air and the recirculating flow at the upper boundary of the oval. Scorer and Davenport[12] derived a model that shows just the opposite, namely detrainment of the vorticity (a consequence of the assumption of constant circulation). Three other models also predict entrainment.[13-15] Tombach[3] and Lissaman et al.[4] thoroughly review the theoretical formulations for the descent of wakes in a stably stratified atmosphere.

An experimental observation that supports the entrainment idea (or at least partial entrainment) is the fact that the vortex pair has been known to descend at nearly constant spacing and finally come to rest at some altitude. To explain this, the concept of entrainment of buoyancy generated circulation must be used in that the internal distribution of the generated vorticity must be such that

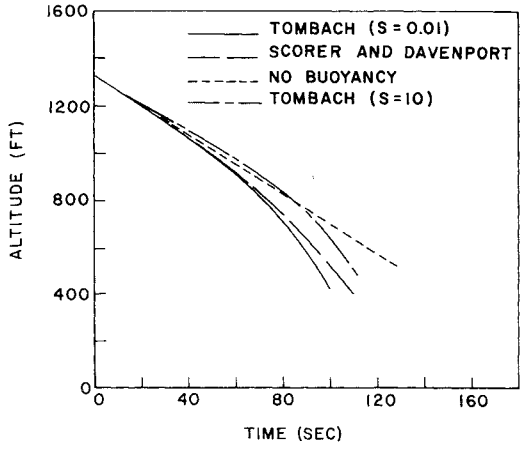

Fig. 9 Altitude vs time in isothermal atmosphere with no shear.

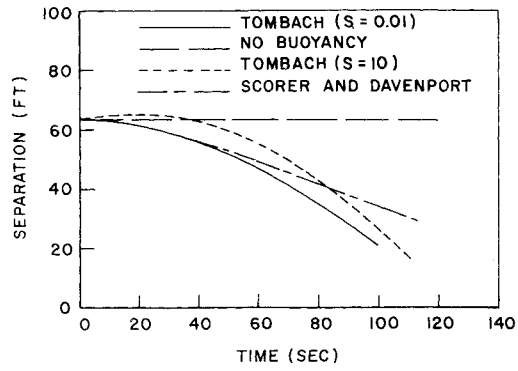

Fig. 10 Separation vs time in isothermal atmosphere with no shear.

the vorticity of one vortex is negated at the location of the other vortex resulting in no induced sink velocity.

The models chosen to represent the effect of buoyancy in the transport model are Tombach's[11] and Scorer and Davenport's.[12] The reasons for choosing these two theories is that a representation of the full spectrum of events is contained in these two models.

A comparison between the two theories is shown in Figs. 9 and 10. In Tombach's model the solution may be generated in terms of an unknown mixing parameter, S(S = 0 corresponds to the Scorer and Davenport model). The effect of buoyancy on the descent is depicted in Fig. 9, where it is seen that for the first minute of life the difference is less than 10%. Figure 10 shows the effect of buoyancy on the separation of the vortex pair. Here the relative difference is somewhat greater (15%) during the first minute.

Vortex Decay, Bursting, and Instability

The inclusion of vortex viscous decay is based on the methods of classical hydrodynamics.[6] A laminar solution for an isolated vortex is obtained from the momentum equation written in terms of the vorticity

$$\zeta = \frac{\Gamma}{4\pi\nu t} e^{-r^2/4\nu t}$$

Replacing the kinematic viscosity ν with the sum of an eddy and kinematic viscosity[18] yields

$$\zeta = \frac{\Gamma}{4\pi(\nu + \epsilon)t} e^{-\frac{r^2}{4(\nu+\epsilon)t}}$$

and the corresponding solution for the circumferential velocity is

$$v = \frac{\Gamma}{2\pi r}\left[1 - e^{-\frac{r^2}{4(\nu+\epsilon)t}}\right]$$

As time increases to infinity, the velocity decreases to zero. However, the vorticity increases from zero up to a maximum value and then asymptotically approaches zero. The circumferential velocity equation is used in the model to calculate a decay using a value of the eddy viscosity obtained from a correlation between the circulation developed by an aircraft and the measured eddy viscosity.[17]

Vortex bursting[18-20] represents a phenomenon that is poorly understood. To date, no satisfactory models are known to exist that can be used for computational purposes. Tombach[3] reports observing (in most cases) vortex bursting over a broad range of atmospheric and flight conditions. The phenomenon manifests itself as a rapid increase in core diameter followed by an axial flow of a conical front. The axial movement can be in either direction or in both directions for the same vortex (at different locations).

To include the Crow type of instability[5] into the model, the vortex core size is calculated using Spreiter and Sacks theory[7] and when the spacing between the vortex pair is equal to the core diameter, breakdown is predicted. This assumes that breakdown occurs upon core contact. (At present, however, there is some thought that an overlap must occur before this happens.[2]) Although the Spreiter and Sacks theory probably predicts vortex core velocities which are too low and core diameters which are too large, it is felt that this represents a relatively good assumption for this application due to its simplicity. Also this assumption does not affect the computed transport of the vortices.

Unification of the Wake Vortex Transport Model

All of the previous mechanisms have been incorporated into a unifying wake vortex transport model. Since the buoyancy models chosen are applicable outside the ground plane region, a transformation altitude is defined to divide the geometric regions of interest into two computational regions. This altitude is normally chosen as 500 ft since at this height the ground plane effects are less than 2% of the transport. A superposition scheme is used to yield an explicit formulation in the velocity domain, while a Runge-Kutta numerical integration is employed in the transport domain.

III. Flight Experiments

Proof-of-concept flight tests were performed at NAFEC during a two-week period in October and November 1972. The tests involved measuring the atmospheric conditions, forecasting the vortex transport, performing the aircraft flybys, and monitoring the vortex tracks. A total of approximately 400 flybys was conducted using DC-6, B-747, B-707, and a CV-880 as the vortex generating aircraft.

The NAFEC Vortex Flight Test Facility consists of a 140-foot tower instrumented with hot-film anemometers, colored smoke dispensers, and meteorological instrumentation. The smoke was used to visualize the vortex tracks (see Fig. 11). A 35-mm camera was located 2000 ft from the tower and normal to the local wind direction. Photographs were taken every second and the tracks were obtained by visually examining each negative in turn and locating the vortex center by scaling photographic distances against known distances.

Supplementing the visual tracks are ground-wind sensor tracks.[22] Propeller anemometers were set out on a baseline near the tower and the passage of a vortex was recorded as a function of time after the aircraft passed.

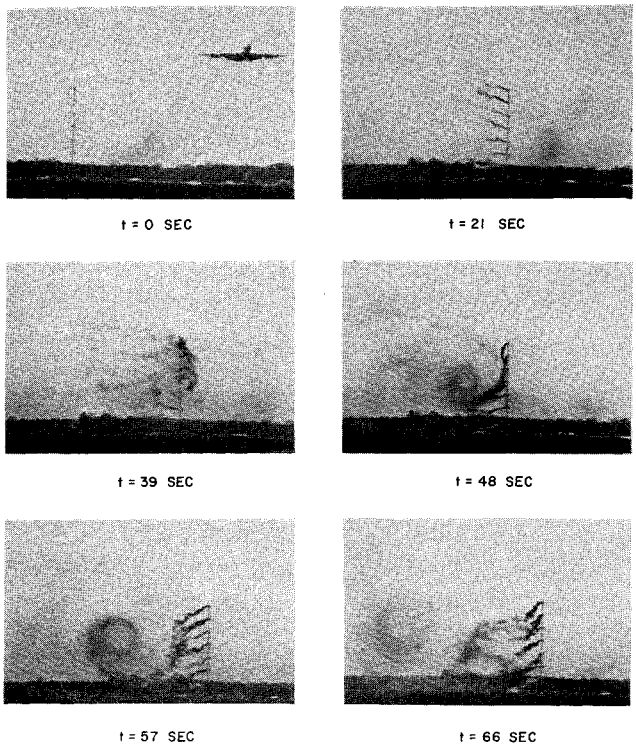

Fig. 11 Typical sequence of tracking photographs (from Ref. 22).

Often the tower smoke dissipated quickly, but the ground-wind sensors were able to extend the range of the visual measurements.

The transport model requires a number of initial conditions. Aircraft configurations, gross weight, velocity, etc., were recorded by the pilots and radioed to the test controller immediately after the aircraft passed the tower. The height and lateral position of the aircraft with respect to the tower were measured by the phototheodolite facilities at NAFEC.

The atmospheric conditions were carefully monitored both before, during, and after the aircraft flybys to accurately determine the conditions during the test and to forecast the vortex transport. Atmospheric variables were recorded from meteorological instrumentation located at five levels on the NAFEC tower (ambient wind velocity, temperature, and relative humidity). The tower data were recorded hourly beginning six hours before the flights to four hours after the flights and continuously during the tests. To test the transport model, two minute averaged data were used to facilitate the quick-look checks which are reported here. The upper air data were monitored by rawinsonde releases to measure the pressure, temperature and winds from the surface (actually around 500 ft MSL) to 5000 ft. The upper air data were recorded hourly beginning three hours before the tests to three hours after the tests were completed.

IV. Predictions vs Experimental Data

At the present time only a relatively small number of the more than 400 flybys have been processed to obtain predictive and experimental tracks. The conclusions reached are tentative and the data presented and discussed are neither the best results obtained to date nor are they the worst results—the cases presented are intended to be considered as representative data.

The results of the first comparison are shown in Fig. 12 for a B-707 flyby. The wind profile used in the analysis was the mean magnitude and direction at each of the five levels on the NAFEC tower averaged over the two min-

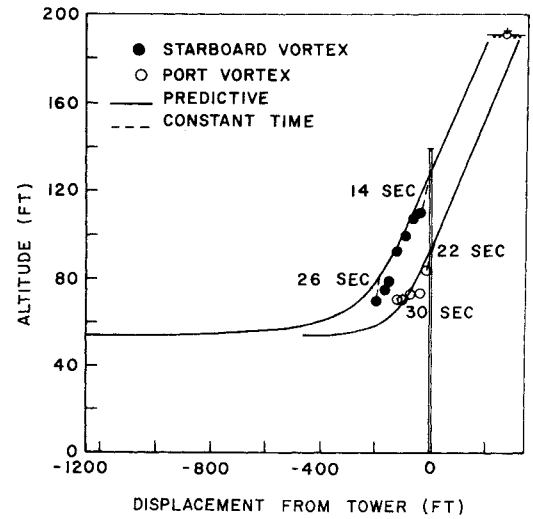

Fig. 12 Comparison between predicted and recorded vortex tracks for a B-707 aircraft flyby.

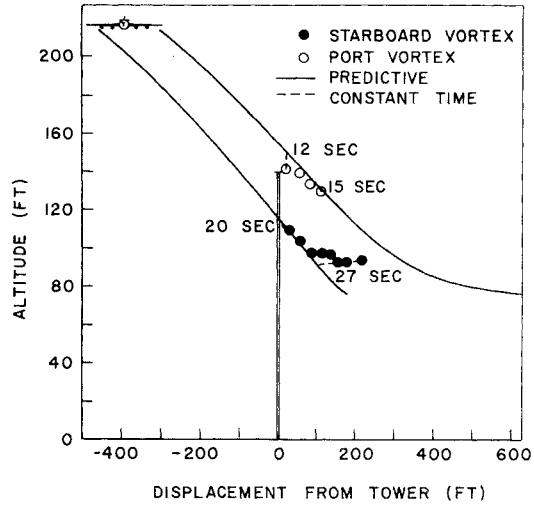

Fig. 13 Comparison between predicted and recorded vortex tracks for a B-747 aircraft flyby.

utes before aircraft passage. The wind profile above the tower was determined by a linear extrapolation from the two highest sensor levels on the tower. The experimental tower hit point occurred at an altitude of 117 ft approximately 13 sec after the aircraft passage for the starboard vortex and at 90 ft and 21 sec for the port vortex. The corresponding predictive hit points are 127 ft at 13.5 sec and 92 ft at 23 sec for the starboard and port vortices, respectively. In general, the disparity in the attitude increases with time (as no vertical velocity was used in the transport model) and ranges from 15 to 20 ft for this run. Note that the separation between the vortices is very close to the theoretical prediction at times up to 26 sec the last experimental data point for the starboard vortex.

A cross-sectional predictive and experimental vortex track is shown in Fig. 13 for one of the B-747 flybys. The port vortex hit the tower 12 sec after aircraft passage and the transport model location estimate at this time is within 7 and 10 ft in the vertical and horizontal distances, respectively. Once again the disparity appears to be due to the linear extrapolation used for the wind profile above the tower. The starboard vortex (second vortex) track location difference between the predictive and experimental data is seen to be less than 10 ft in the vertical and less than 20 ft in lateral position at the tower hit time of

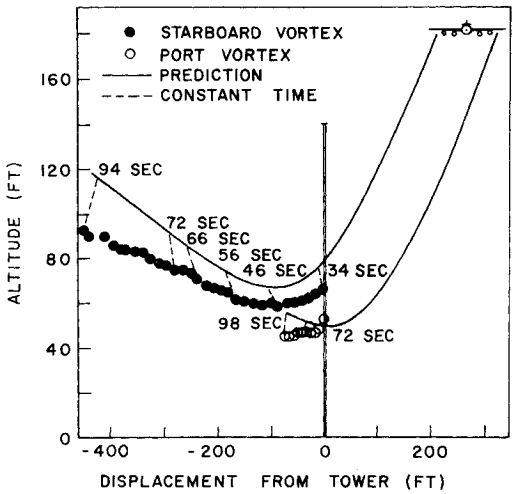

Fig. 14 Comparison of predictive (including wind shear) and recorded vortex tracks for a B-707 aircraft flyby.

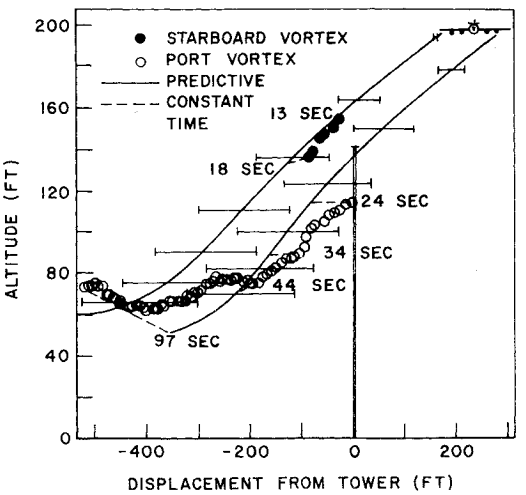

Fig. 15 Comparison between predicted and recorded vortex tracks for mean wind with plus and minus one standard deviation effects for a B-707 aircraft flyby.

20 sec; as time increases the difference between the measured and predicted altitude decreases while the difference in the measured and predicted lateral position increases. Note that the cross wind is just sufficient to negate the upwind movement of the starboard vortex in the predictive track. Thus the actual lateral position is very sensitive to the temporal wind field for this magnitude of mean cross wind.

An example of a larger difference between the predictive and experimental tracks can be seen in Fig. 14. Note that the vortex is rising. A mean wind profile with shear was originally used to determine the predictive tracks but this resulted in predictive tower hits higher and earlier in time than the experimental values. However, the value of the mean wind for the run at the 100-ft level was considerably less than the 70-ft level and since only the 100- and 140-ft levels are used to extrapolate the mean wind to altitudes above the tower, a cross wind is computed that could be in error. This could easily account for the earlier and higher tower hits. In addition, the wind profile for this run (actually the two minutes just before aircraft arrival) is very blunt compared to a normal profile. In fact the mean velocity plus one standard deviation at the 23-ft level is greater than the mean plus one standard deviation at the 100-ft level and is also greater than the mean at 140 ft implying a significant shear layer near the ground. The wind shear technique previously discussed was used to examine the effect and the results are shown in Fig. 14 (where all the vorticity was concentrated in one row). The inclusion of shear both predicts the correct trend of the motion and greatly improves the horizontal location disparity. Both vortices still show predicted altitudes greater than the experimental values. However, the expected error in the high altitude wind profile probably is contributing to the lack of agreement between the transport model prediction and the measured vortex attitude.

Before performing a detailed sensitivity analysis of all of the parameters involved, it is instructive to investigate the consequences of the uncertainties in the wind field. A series of three predictive tracks has been generated for each flyby, one corresponding to the mean wind profile and the other two representing plus and minus one standard deviation. One such case is shown in Fig. 15. It is seen that the mean profile is somewhat above the experimental points for both vortices. Perhaps this may again be accounted for by the crude linear extrapolation technique used to calculate the wind profile above the NAFEC tower. In any event it is seen that the $\pm 1\sigma$ predictive tracks bound the data for times up to 70 sec.

One technique for generating predictive tracks is to use the first photographic data point as the initial conditions for the transport model. The higher altitude wind profile problems previously discussed are alleviated and a more meaningful parametric analysis can be obtained. Tentative results indicate that in general a better predictive track results. It is believed that after the wind profile technique is improved the same conclusion obtained from the parametric analysis can be applied to the tracks initiated at the actual aircraft location rather than at first sighting.

Further Tests

In early 1974, TSC will be conducting an extensive series of tests at the John F. Kennedy International Airport. The approach zone of runway 31R will be monitored with a number of vortex tracking systems (a pulsed bistatic acoustic system,[23,24] a CW bistatic acoustic system,[25] a ground-wind system[26] similar to the one used in the NAFEC tests, and a CW CO_2 Doppler laser[26] data system). The two primary objectives of the test program will be the evaluation of the vortex sensors and the validation of the vortex transport and lifetime models for forecasting the behavior of the vortex sensors and the validation of the vortex transport and lifetime models for forecasting the behavior of the vortex wakes. A network of tower-mounted meteorological sensors will be used to continuously monitor the three components of the wind, turbulence, temperature, and humidity at a number of stations on each tower. The test period will extend over about 10 months thus allowing a large data base to be collected ensuring that many different weather conditions will be examined.

Conclusions

The separation standards for "nonheavy" aircraft following "heavy" aircraft were implemented to reduce the probability of a hazardous vortex encounter. For most meteorological conditions, the 5-mile spacing is conservative and reduces air terminal capacities. This approach is in direct contrast to the projected needs for airport capacity. These considerations served as the impetus for analyzing the feasibility of a Wake Vortex Avoidance System.

An integral part of a Wake Vortex Avoidance System is the predictive capability discussed in this paper for forecasting the transport of the vortices in the terminal environment. The results discussed in this paper (although

tentative) indicate the feasibility of predicting vortex transport. It is realized that many more comparisons between predictive and experimental tracks are needed and are forthcoming. A summary of the major conclusions which can be made at the present time include: 1) Establishment of the feasibility of predicting the transport of aircraft wake vortices. 2) Establishment of the importance of the atmospheric wind field on the transport of the vortices. 3) Unification of simple models describing the physics of the important mechanisms into a wake vortex transport algorithm.

References

[1]Gorstein, M., Hallock, J., and McWilliams, I., "Aircraft Wake Vortex Avoidance Systems," *EASTCON-72 Proceedings,* Oct. 1972.

[2]Wilson, D. J., Brashears, M. R., Carter, E. A., and Shrider, K. R., "Wake Vortex Predictive System," Rept. FAA-RD-72-108, Dec. 1972. Lockheed Missiles & Space Company, Inc., Also a summary presented at Accident Prevention Forum on Aircraft Approaches and Landings, National Transportation Safety Board, Oct. 1972, Washington, D.C.

[3]Tombach, I. H., "Observations of Atmospheric Effects on the Transport and Decay of Trailing Vortex Wakes," AIAA Paper 73-118, Washington, D.C., 1973.

[4]Lissaman, P. B. S., Crow, S. C., MacCready, P. B., Tomach, I. H., and Bate, E. R., Jr., "Aircraft Vortex Wake Descent and Decay Under Real Atmospheric Effects," Rept. FAA-RD-73-120, AeroVironment, Inc., Pasadena, Calif., Oct. 1973.

[5]Crow, S. C., "Stability Theory for a Pair of Trailing Vortices," *AIAA Journal,* Vol. 8, No. 12, Dec. 1970, pp. 2172.

[6]Lamb, H., *Hydrodynamics,* Dover, New York, 1945.

[7]Spreiter, J. R. and Sacks, A. H., "The Rolling Up of the Trailing Vortex Sheet and its Effect on the Downwash Behind Wings," *Journal of Aerospace Sciences,* Vol. 18, No. 1, Jan. 1951, pp. 21–32.

[8]Harvey, J. K. and Perry F. J., "Flow Field Produced by Trailing Vortex in the Vicinity of the Ground," *AIAA Journal,* Vol. 10, No. 8, Aug. 1971, p. 659.

[9]Burnham, D. C., "Effect of Ground Wind Shear on Aircraft Trailing Vortices," *AIAA Journal,* Vol. 10, No. 8, Aug. 1972, p. 1114.

[10]Prandtl, L. and Tietjens, O. G., *Fundamentals of Hydro- and Aeromechanics,* Dover, New York, 1957, p. 194.

[11]Tombach, I. H., "Transport of a Vortex Wake in a Stably Stratified Atmosphere," *Aircraft Wake Turbulence and Its Detection,* edited by J. H. Olsen et al., Plenum Press, 1971, pp. 41-56.

[12]Scorer, R. S. and Davenport, L. J., "Contrails and Aircraft Downwash," *Journal Fluid Mechanics,* Vol. 43, 1970, pp. 451–464.

[13]Tulin, M. P. and Shwartz, J., "The Motion of Turbulent Vortex-Pairs in Homogeneous and Density Stratified Media," TR 231-15, AD 723 187, Hydronautics, Inc., Laurel, Md., 1971.

[14]Saffmann, P. G., "The Motion of a Vortex Pair in a Stratified Atmosphere," *Studies in Applied Mathematics,* Vol. 51, 1972, pp. 107–119.

[15]Kuhn, G. D., and Nielsen, J. H., "Analytical Studies of Aircraft Trailing Vortices," AIAA Paper 72-42, San Diego, Calif., 1972.

[16]Squire, H. D., "The Growth of a Vortex in Turbulent Flow," *Aeronautical Quarterly,* Vol. 16, Aug. 1965, pp 302–306.

[17]Owen, P. R., "The Decay of a Turbulent Trailing Vortex," *Aeronautical Quarterly,* Vol. 21, Feb. 1970, pp. 69–78.

[18]Benjamin, T. B., "Theory of Vortex Breakdown Phenomena," *Journal of Fluid Mechanics,* Vol. 14, No. 4, 1962, pp. 543–629.

[19]Harvey, J. K., "Some Observations of the Vortex Breakdown Phenomena," *Journal of Fluid Mechanics,* Vol. 14, No. 4, 1962, p. 629.

[20]Ludwieg, H., "Zur Erklarung des Instabilitat des uber Angestellten Deltaflugeln Auftretenden Freien Werkelkerne," *Zeitschrift fur Hugurssen Schaften,* Vol. 10, 1962, p. 242.

[21]Moore, D. W. and Saffman, P. G., "Structure of a Line Vortex in an Imposed Strain," *Aircraft Wake Turbulence and Its Detection,* edited by J. H. Olsen et al., Plenum Press, New York, 1971.

[22]Sullivan, T. and Burnham, D. C., "Preliminary Report, Calibration of Wake Vortex Sensors at NAFEC," to be published.

[23]Burnham, D. C., Hallock, J. N., Kodis, R., and Sullivan, T., "Vortex Sensing Tests at NAFEC," TR DOT-TSC-FAA-72-7, Jan. 1972, DOT/Transportation Systems Center, Cambridge, Mass.

[24]Sullivan, T., Burnham, D. C., and Kodis, R., "Vortex Sensing Tests at Logan and Kennedy Airports," TSC Rept. FAA-RD-72-141, Dec. 1972,

[25]Balser, M., Nagy, A. E., and McNary, C., "Acoustic Analysis of Aircraft Vortex Characteristics," Rept. FAA-RD-72-81, July 1972, Xonics Rept. to Federal Aviation Administration, Washington, D.C.

[26]Lawrence, T. R., Wilson, D. J., Craven, C. E., Jones, I. P., Huffaker, R. M., and Thomson, J. A. L., "A Laser Velocimeter for Remote Wind Measurements," Review of Scientific Instruments, No. 43, 1972, p. 512.